IOP Conference Series: Materials Science and Engineering

PAPER • **OPEN ACCESS**

Finite element analysis on contact stress of high-speed railway bearings

To cite this article: K Yang *et al* 2019 *IOP Conf. Ser.: Mater. Sci. Eng.* **504** 012073

View the article online for updates and enhancements.

This content was downloaded from IP address 108.61.201.231 on 14/10/2019 at 02:22

Finite element analysis on contact stress of high-speed railway bearings

K Yang, G Zhang*, Y W Wang and S Cai

Research Institute Mechanical design and Bearing, School of Mechatronic Engineering and Automation, Shanghai University, Shanghai 200072, China

Corresponding author and e-mail: G Zhang, zg@shu.edu.cn

Abstract. In the process of structural design and fatigue life analysis of the high-speed railway bearing, the calculation of the contact stress between the roller and the raceway is an important element. At first, this paper solved the contact load distribution of the two rows of rollers of the high-speed railway bearing under the action of radial and axial forces, to determine the roller which carried the maximum contact load, and calculated the surface contact stress distribution and the subsurface stress distribution between the roller and the raceway. Then, this paper made use of the good data interface between SOLIDWORKS and ANSYS Workbench, used SOLIDWORKS to set up the structural model of the high-speed railway bearing, and imported it into ANSYS Workbench for finite element analysis. Finally, by comparing the simulation results with the results of traditional theoretical calculation, the correctness of the finite element analysis is proved, which provides scientific basis for the design, manufacture and the fatigue life analysis of high-speed railway bearings.

1. Introduction

With the development of science and technology, efficient and convenient high-speed railway trains have become an important means of transportation between cities. High-speed railway trains refer to trains running at a speed of over 300km/h [1]. The high-speed railway bearing is one of the important components of high-speed railway train operation. Its fatigue life and service performance directly affect the stability and safety of the high-speed railway vehicle [2]. Under the condition that the bearing is installed correctly, the seal is normal, and the lubrication is good, the failure of most high-speed railway bearings is contact fatigue damage, which is caused by the excessive contact stress between the roller and the raceway, so it is necessary to study the surface contact stress distribution and subsurface stress distribution of the high-speed railway bearing.

At present, high-speed railway bearings are mostly double-row tapered roller bearings [1-2]. During the operation of the high-speed railway bearing, the two rows of tapered rollers of the bearing must be loaded, and the loading conditions are different. Because of the special structure of the bearing, the calculation method of the bearing is different from the traditional rolling bearing. J S Yan et al. [3] established a quasi-dynamic model of high-speed railway bearing, and analyzed the influence of external working condition on load distribution of the bearing. L Y Zhang et al. [4] took the tapered roller of high-speed railway bearing as the research object, and used the finite element method to study the influence of different convex and convex metrics on the contact stress between the roller and the raceway. Nayak L et al. [5] calculated the relationship between the maximum contact load and the

Content from this work may be used under the terms of the Creative Commons Attribution 3.0 licence. Any further distribution of this work must maintain attribution to the author(s) and the title of the work, journal citation and DOI.
Published under licence by IOP Publishing Ltd

radial load applied to the rolling elements of the bearing. Poplawski J V et al. [6] calculated the contact stress of the cylindrical roller bearing under different roller profiles, and predicted its fatigue life by using contact stress. Z S Guo et al. [7], Z W Wang et al. [8] studied the finite element method for the contact stress of rolling bearings, and proved the correctness of the method. M Y Wang et al. [9] and H Y Shu et al. [10] carried out finite element analysis on tapered roller bearings, explored the stress distribution law in contact areas of the bearing, and sought the optimal convexity design of the logarithmic roller.

However, the above studies mainly focused on the theoretical calculation and finite element simulation analysis on contact stress of rolling bearing, or the influence of tapered roller with different convexity on contact stress of the bearing. There is no finite element analysis on contact stress of the double-row tapered roller bearing under the action of a certain external load. Therefore, this paper carries out traditional theoretical calculation and finite element analysis on contact stress of high-speed railway bearing under the action of a certain radial and axial forces, and compares the two results with each other to prove the correctness of the finite element analysis. It provides scientific basis for structural design and fatigue life analysis of the high-speed railway bearing.

2. Structure and basic parameters of high-speed railway bearings

The axle box bearing of the high-speed railway train studied in this paper is double-row tapered roller bearing, which consists of inner ring, outer ring, rolling elements and cage. The inner ring usually fits tightly with the shaft and rotates with the shaft. The outer ring generally cooperates with the inner wall of the axle box to act as a support. The rolling elements are uniformly arranged between the inner and outer rings by means of a cage, whose shape, size and number directly determine the load carrying capacity of the bearing. At the same time, the cage separates the rolling elements evenly and guides the rolling elements to move on the correct track [3].

During the actual operation, the high-speed railway bearing not only bears large radial load, but also has to bear a certain extent of axial load. This paper takes a high-speed railway bearing with a radial force of 86KN, an axial force of 17KN and model LY-Z028 as an example. The structural diagram and sectional view of the bearing are shown in Figure 1 and Figure 2 respectively, and the specific structural parameters are shown in Table 1.

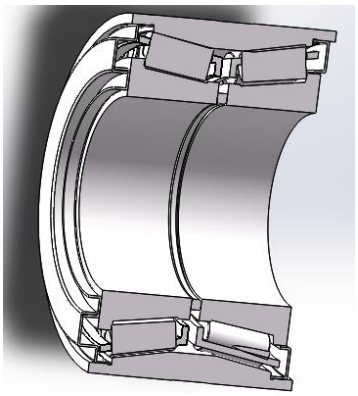

Figure 1. Structural diagram of high-speed railway bearing.

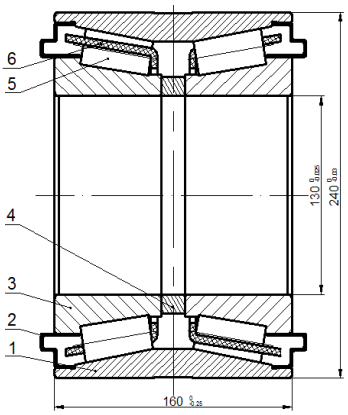

1 -Outer Ring 2 - Dust Cover
3 - Inner Ring 4 -Spacer 5 - Roller
6 – Cage

Figure 2. Sectional view of high-speed railway bearing.

Table 1. Structural parameters of high-speed railway bearing.

Parameter	Value
Nominal outer diameter D(mm)	240
Nominal bore diameter d(mm)	130
Width of bearing T(mm)	160
Small end diameter of roller D_{min}(mm)	22
Large end diameter of roller D_{max}(mm)	24
Mean diameter of roller D_m(mm)	23
Pitch circle diameter of bearing d_m(mm)	185
Contact angle of inner ring α_i(°)	7°45′
Contact angle of outer ring α_o(°)	10
Length of roller L(mm)	50
Number of rollers Z	2×17
Half cone angle of roller ϕ(°)	1°12′30″
Effective length of roller l(mm)	45

3. Contact analysis of bearings

Contact analysis is a typical nonlinear problem in finite element analysis. It is a highly nonlinear behavior that requires more computational resources. There are two major difficulties in the contact problem: First, before the problem is solved, the range of the contact area is unclear, and the contact or separation between the surfaces is unknown, and the contact area varies with load, material, boundary conditions, and other factors; Second, the contact problem often requires the calculation of friction, and all friction models are nonlinear, making the problem more difficult to converge [5].

It often encounters some problems related to bearing capacity, fatigue life, deformation and stiffness in the design and application analysis of rolling bearings, and these issues are closely linked with the force and stress distribution in the bearing [6]. Therefore, it is very important to conduct contact analysis for bearings. The surface contact stress and subsurface stress of the high-speed railway bearing under the combined action of radial and axial loads are analyzed in this paper, which provides a basis for the analysis of fatigue life of high-speed railway bearings.

4. Stress calculation of high-speed railway bearings

4.1. Surface contact stress

During operation, the high-speed railway bearing will bear large radial load and certain axial load. Due to the unique geometric relationship of taper roller bearing, the load will be redistributed among the various rollers under the action of external load. In addition, under high-speed condition, the centrifugal force will affect load distribution of the bearing. Therefore, it is necessary to solve the load distribution of two rows of rollers, to determine the roller which bears the maximum force, to find the maximum contact stress by using Hertz contact theory, and to lay the foundation for the subsequent finite element analysis.

In the case of ignoring the friction torque and the oil film force, when the bearing is running steadily, it is considered that the forces of the rollers are balanced, and the forces of the single roller are shown in Figure 3:

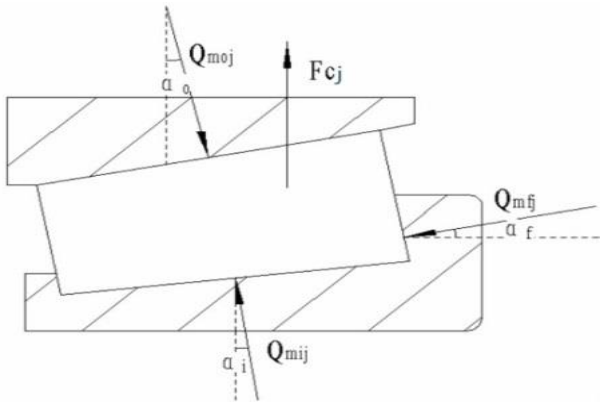

Figure 3. Force analysis of single roller.

The force balance equations of a single roller are:

$$Q_{mij}\sin\alpha_i + Q_{mfj}\cos\alpha_f - Q_{moj}\sin\alpha_o = 0 \tag{1}$$

$$Q_{mij}\cos\alpha_i + F_{cj} - Q_{moj}\cos\alpha_o - Q_{mfj}\cos\alpha_f = 0 \tag{2}$$

Here, Q_{mij} , Q_{moj} represent the positive pressure of the inner and outer rings of the bearing on the roller respectively, Q_{mfj} represents the positive pressure of the inner ring rib on the large end face of the roller, F_{cj} represents the centrifugal force of the roller, α_i ,α_o are contact angles of inner and outer rings respectively, α_f is the contact angle between the inner ring rib and the large end face of the roller, and the subscript m is the serial number of two rows of rollers, m=1, 2, and j is the serial number of the rollers, j=1-17.

The centrifugal force of the roller rotating around the axis of the bearing at a revolution speed of n_m is:

$$F_{cj}=3.39\times10^{-11}\bullet D_m^2 l d_m n_m^2 \tag{3}$$

Where D_m is the mean diameter of the roller, l is the effective length of the roller, and d_m is the pitch circle diameter of the bearing. For the tapered roller bearing with small cone angle, according to Hertz contact theory, the relationship of the contact load and deformation between the roller and outer ring can be obtained:

$$Q_{moj}=K\delta_{mnj}^{1.11} \tag{4}$$

$$K=8.06\times10^4 l^{8/9} \tag{5}$$

Where K is the contact stiffness coefficient between the roller and the outer ring, δ_{mnj} is the size of the contact deformation between the roller and the outer ring, and *n* represents the normal direction of the roller contact line. When calculating the size of the contact deformation between the roller and the outer ring, the two inner rings of the double-row tapered roller bearing are considered as a whole, so that the total radial and axial displacements of the inner ring relative to the outer ring are respectively δ_r and δ_a. Ignoring the bending deformation of the inner and outer rings of the bearing, the position where the azimuth angle of the roller is $\varphi_j = 0$ is defined along the direction of the radial force F_r in

Figure 4. At the roller whose azimuth angle is φ_j, The total displacements in the direction of the outer ring contact normal are:

$$\delta_{1nj} = \delta_r \cos\varphi_{1j} \cos\alpha_o + \delta_a \sin\alpha_o \tag{6}$$

$$\delta_{2nj} = \delta_r \cos\varphi_{2j} \cos\alpha_o - \delta_a \sin\alpha_o \tag{7}$$

When calculating the contact loads between outer ring and rollers, not all rollers bear the loads, so it should be determined during calculation. If $\delta_{mnj} \le 0$, the contact loads between outer ring and rollers are zero.

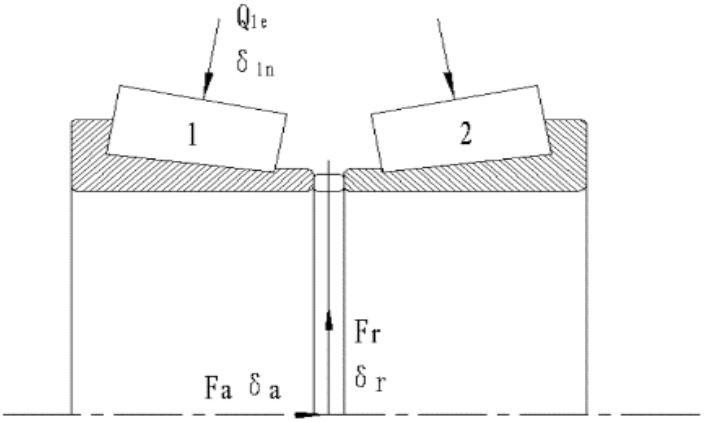

Figure 4. Force diagram of inner ring - roller of the bearing.

Still, the position where the azimuth angle of the roller is $\varphi_j = 0$ is defined along the direction of the radial force F_r in Figure 4, and the force balance equations of the overall bearing can be obtained:

$$F_r = \sum_{m=1}^{2} \sum_{j=1}^{Z} Q_{moj} \cos\alpha_o \cos\varphi_{mj} \tag{8}$$

$$F_a = \sum_{m=1}^{2} \sum_{j=1}^{Z} Q_{moj} \sin\alpha_o \tag{9}$$

Where Z is the number of rollers, F_r is the radial load on the bearing, and F_a is the axial load on the bearing. The above equations (1) to (9) are combined to obtain the contact loads Q_i, Q_o, and Q_f between the roller and the raceway by using the least square method for multiple iterations.

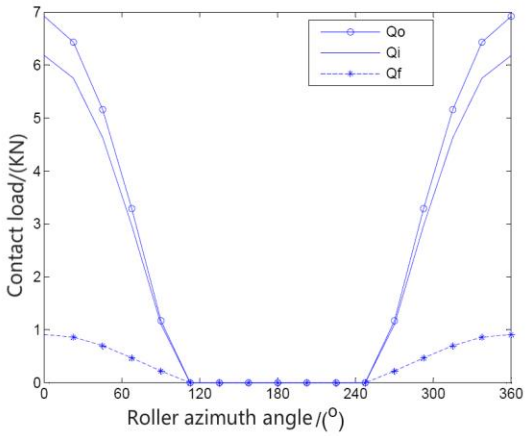

Figure 5. Load distribution of the first row of rollers.

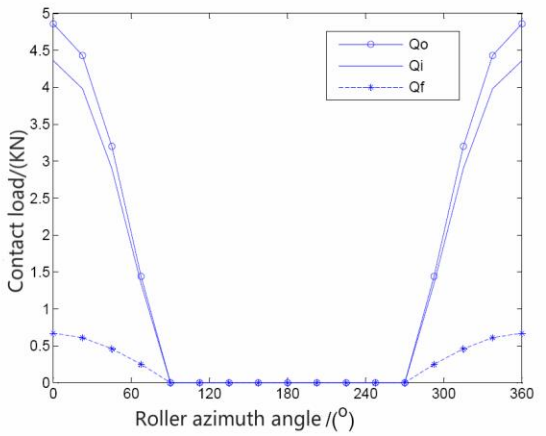

Figure 6. Load distribution of the second row of rollers.

When the train is running at 350km/h and the bearing bears with radial force of 86kN and axial force of 17kN, the contact load distribution of the first and second row of rollers with the inner ring, the outer ring and the inner ring rib are shown in Figure 5 and Figure 6 where Q_i is with the inner ring, Q_o is with the outer ring and Q_f is with the inner ring rib respectively. Comparing Figure 5 and Figure 6, it can be seen that the maximum contact load of the first row of rollers is 1.4 times the maximum contact load of the second row of rollers, so the first row of rollers bear most of the load. Therefore, the roller that bears the maximum contact load in the first row of rollers is taken as the roller that receives the maximum stress, that is, the roller whose azimuth angle is $\varphi = 0$, and the contact load between the roller and the outer ring is 6.92KN.

In the case where the contact angle of the tapered roller is small, according to the Hertz contact theory, the maximum contact stress $\sigma_{\max}$ between the tapered roller and the raceway and the half width b of the contact surface can be approximately expressed as [11]:

$$\sigma_{\max} = \frac{2Q}{\pi l b} \tag{10}$$

$$b = 3.35\times10^{-3}\left(\frac{Q}{l\sum\rho}\right)^{1/2} \tag{11}$$

Combining equations (10) and (11), the maximum contact stress of the bearing can be found to be 742.13MPa. Figure 7 is the contact stress distribution when the contact load between the roller and the raceway is 6.92KN.

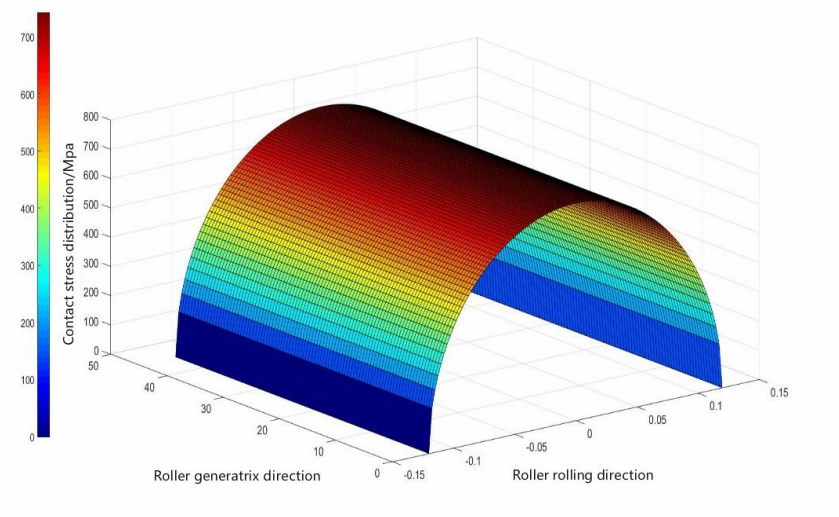

Figure 7. Contact stress distribution of roller- raceway with contact load of 6.92KN.

4.2. Subsurface stress

The fatigue life of the high-speed railway bearing is long, and bearing failure originates from less surface damage. Most bearings failures often originate from some points under the contact surface. Therefore, it is necessary to solve the stress distribution under the contact surface, that is, the subsurface stress distribution, and to find the maximum subsurface stress is of significance.

In order to better express the cause of bearing failure, The Von Mises stress can be used as a measure of failure criteria. Von Mises stress is calculated as:

$$\sigma_V = \left\{ \frac{1}{2} \left[\left(\sigma_x - \sigma_y \right)^2 + \left(\sigma_y - \sigma_z \right)^2 + \left(\sigma_z - \sigma_x \right)^2 + 6\left(\tau^2_{xy} + \tau^2_{yz} + \tau^2_{zx} \right) \right] \right\}^{1/2} \tag{12}$$

Where σ_x, σ_y and σ_z are the normal stresses along the x, y and z directions of the roller respectively, and τ_{xy}, τ_{yz} and τ_{zx} are shear stresses along the x, y and z directions of the roller respectively.

In the plane strain state, the non-zero stress components are σ_x, σ_y , σ_z and τ_{zx}. So, Von Mises stress is:

$$\sigma_V = \left\{ \frac{1}{2} \left[\left(\sigma_x - \sigma_y \right)^2 + \left(\sigma_y - \sigma_z \right)^2 + \left(\sigma_z - \sigma_x \right)^2 + 6\tau^2_{zx} \right] \right\}^{1/2} \tag{13}$$

When the roller is in contact with the bearing ring, it is assumed that the bearing ring is an elastic semi-infinite body. By using the elastic Hertz contact theory, the formulas for calculating the internal stress of an object are [7]:

$$\sigma_x = -\frac{\sigma_{\max}}{b} \left\{ m \left(1 + \frac{z^2 + n^2}{m^2 + n^2} \right) - 2z \right\} \tag{14}$$

$$\sigma_y = \mu \left(\sigma_x + \sigma_z \right) \tag{15}$$

$$\sigma_z = -\frac{\sigma_{\max}}{b} m \left(1 - \frac{z^2 + n^2}{m^2 + n^2} \right) \tag{16}$$

$$\tau_{zx} = -\frac{\sigma_{\max}}{b} n\left(\frac{m^2 - z^2}{m^2 + n^2}\right) \tag{17}$$

Where μ is the Poisson's ratio of the material, $\mu = 0.3$. The formulas for m^2 and n^2 are:

$$m^2 = \frac{1}{2}\left[\sqrt{\left(b^2 - x^2 + z^2\right)^2 + 4x^2z^2} + \left(b^2 - x^2 + z^2\right)\right] \tag{18}$$

$$n^2 = \frac{1}{2}\left[\sqrt{\left(b^2 - x^2 + z^2\right)^2 + 4x^2z^2} - \left(b^2 - x^2 + z^2\right)\right] \tag{19}$$

Figure 8 shows the Von Mises stress distribution in the subsurface between the roller subjected to the maximum contact load and the raceway, which was calculated by MATLAB programming. It can be seen from Figure 8 that the Von Mises stress is symmetrically distributed about the load acting line, and the maximum Von Mises stress is also located on the load acting line: at z = 0.092mm, the Von Mises stress reaches its maximum and the maximum is 544.903MPa.

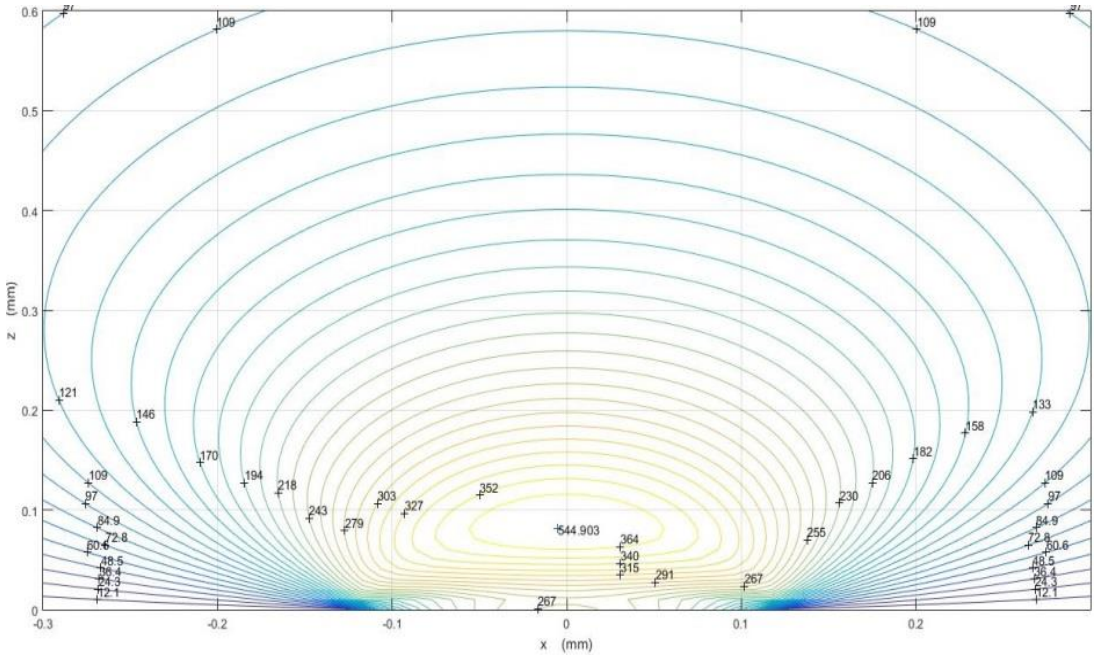

Figure 8. Contour map of Von Mises stress.

5. Finite element analysis

5.1. Establishment of a finite element model

This paper makes use of the good data interface between SOLIDWORKS and ANSYS Workbench, uses SOLIDWORKS to set up the structural model of the high-speed railway bearing and imports it into ANSYS Workbench for finite element analysis. Considering that the overall analysis of high-speed railway bearing takes a long time and is difficult to solve, the general conclusion can be obtained only by finite element analysis on the roller subjected to the maximum contact load. In addition, the larger the model, the coarser the mesh will be, and the larger the error will be. Considering the symmetrical distribution of the contact stress, half of the roller and the inner and outer rings can be analyzed. According to the above analysis, a roller in the first row of rollers is subjected to the maximum contact load, so half of its model is taken out separately for finite element analysis.

Before the finite element analysis on the contact stress of high-speed railway bearing, the factors that have little influence on the analysis process are ignored according to the force condition of the bearing:

(1) The high-speed railway bearing has less plastic deformation during the actual contact, so it is assumed that the deformation of the bearing is within the range of elastic deformation.

(2) When the bearing is actually working, it is approximately in a zero clearance state, and for the convenience of modeling, it is handled according to zero clearance [8].

(3) In order to avoid calculation difficulties, to simplify the model, we ignore some structural factors such as chamfering and small holes.

(4) In order to simulate the cooperation between the outer ring of the bearing and the bearing seat, the outer ring of the bearing is fixed without considering the influence of the bearing seat on the bearing [9].

(5) Ignore the influence of friction torque.

The three-dimensional geometric model is imported, as shown in Figure 9. The material is set to GCr15 with a density of $7.83\times10^{3}kg/m^{3}$, an elastic modulus of 219GPa, and a Poisson's ratio of 0.3.

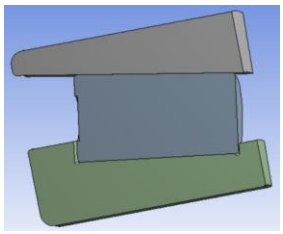

Figure 9. Finite element model.

5.2. Meshing

The quality and density of meshing have a direct impact on the results of finite element analysis. It is necessary to fully consider the size of the model, the speed of calculation, and the accuracy of the results. In general, the denser the mesh is, the higher the accuracy of the result, but when the mesh is too dense, it makes the solution very difficult. Therefore, it is very important to choose the appropriate density of the mesh [12]. Here, the mesh is divided by means of intelligent first-level subdivision and the mesh is refined in the contact area. As shown in Figure 10, the number of finite element units generated is 38765, and the number of nodes is 66056.

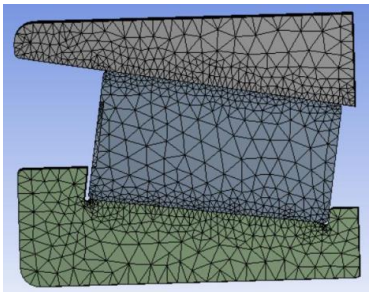

Figure 10. Map of meshing.

5.3. Contact pair setting

The outer surface of the roller is selected as the target surface, and the surface of the inner and outer rings raceways in contact with the roller is selected as the contact surface, so that a corresponding contact pair can be established. The size of penetration between the two surfaces depends on the contact stiffness and is negatively correlated with the contact stiffness. Excessive contact stiffness may cause morbidity in the total stiffness matrix, which leads to difficulties in convergence. Therefore, the

large enough contact stiffness should be selected to ensure that the contact penetration is small enough to be acceptable. At the same time, the contact stiffness should not be so large as to cause morbidity in the total stiffness matrix and ensure its convergence [10]. This article sets a normal stiffness factor of 0.01. The gap is closed by small adjustments, and forcing the initial contact to be closed at the beginning of the analysis.

5.4. Applying constraints and loads

The outer ring of the high-speed railway bearing is fixed and the inner ring rotates. Therefore, a fixed constraint is imposed on the outer surface of the outer ring, and a load is applied at the contact between the inner ring raceway and the roller. At the same time, a symmetric constraint is imposed on the divided faces of the inner and outer rings. Activate the large deformation option and close the weak spring. Set the solution time to 1s, the number of substeps to 100, the minimum number of substeps to 10, the maximum number of substeps to 1000, and turn on the automatic time step.

5.5. Solving

The solving process is the same as the general nonlinear solving process. After reading the results, we can view the information including displacement, stress, strain and so on. Figure 11 shows the contact stress distribution, and Figure 12 shows the Von Mises stress distribution.

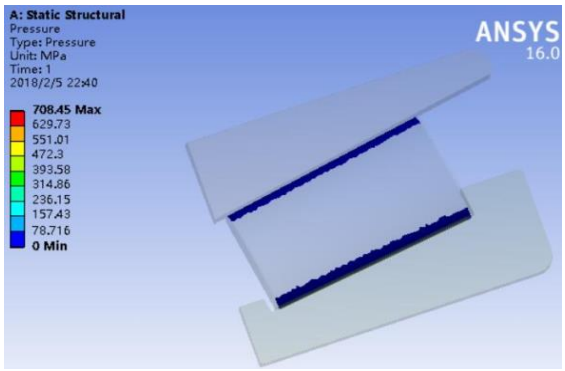

Figure 11. Contact stress distribution.

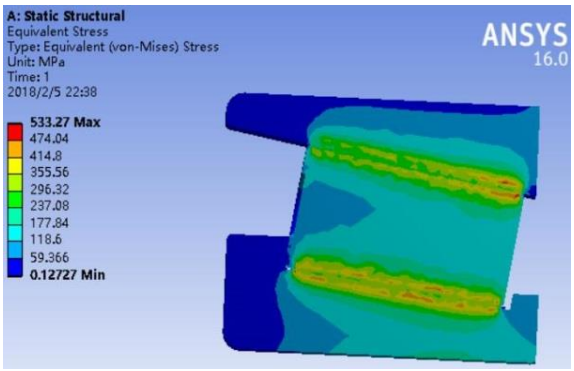

Figure 12. Von Mises stress distribution.

From Figures 11 and 12, it can be seen that the maximum contact stress between the roller and the raceway is 708.45MPa, and the maximum Von Mises stress which is at a certain depth below the contact surface of the roller is 533.27MPa. Under the action of the load, the contact stress and the Von Mises stress of the bearing are symmetrically distributed about the load acting line. The stress between the roller and the raceway is evenly distributed in the middle, decreasing from the middle to both sides, and the maximum stress appears on the load acting line, which is in accordance with the previous theoretical calculations.

5.6. Analysis of results

As can be seen from Table 2, the values of traditional theoretical calculation are greater than the finite element analysis values, indicating that the values of traditional theoretical calculation are relatively safe. The values of traditional theoretical calculation and the finite element analysis values are basically the same, and the relative error is small, within the allowable range of the engineering errors. The two maximum contact stresses do not exceed the allowable contact stress, and the two maximum Von Mises stress do not exceed yield limit σ_s and tensile strength limit σ_b of the material, so the bearing is safe. It can be seen that it is feasible to replace traditional theoretical calculation with finite element simulation analysis, and the finite element analysis values are closest to the experimental values [5-6,11].

Table 2. Comparison between the values of traditional theoretical calculation and the finite element analysis values.

	Theoretical values /MPa	Finite element analysis values /MPa	Relative error /%	Allowable contact stress /MPa	
Contact stress	742.13	708.45	4.75	2700	
Von Mises stress	544.903	533.27	2.2	σ_b	σ_s
				1080	930

6. Conclusions

In this paper, the finite element analysis method is used to solve contact stress of the high-speed railway bearing under the combined action of radial and axial loads. It can be known from the analysis results that the high-speed railway bearing is safe under this working condition.

Compared to using traditional theoretical calculation method to solve contact stress of the high-speed railway bearing, the finite element analysis method is more convenient and faster, and does not require cumbersome mechanical calculations. The finite element analysis results are basically consistent with the traditional theoretical calculations.

The finite element analysis on contact stress can truly reflect the stress distribution between the roller and the raceway of the high-speed railway bearing, providing scientific basis for the design, manufacture and the fatigue life analysis of the high-speed railway bearing.

However, the solution to contact stress of the high-speed railway bearing is limited to the bearing which bears a certain radial and axial loads, without considering the torque generated by the high-speed railway train in the process of turning. In addition, during the actual operation of the high-speed railway bearing, the axial load sometimes changes. The influence of the change of axial load on the contact stress of the high-speed railway bearing will also be the subject that we will study next.

Acknowledgement

The authors are very grateful for the support by the Key Project of Natural Science Foundation of China (U1560202).

References

[1] Yang X W 2011 *Bearing* vol 10 pp 59-61
[2] Sun Z H 2004 *Rolling Stock* vol 42 No.8 pp 4-7
[3] Yan J S, Zhu L Q, Zhao S X, Song S Y, Wang F C 2012 *Bearing* vol 10 pp 12-16
[4] Zhang L Y, Xue Y J, Niu Q B, Ye J 2014 *Machinery Design and Manufacture* vol 9 pp 72-77
[5] Nayak L, Johnson K L 1979 *International Journal of Mechanical Sciences* vol 21 pp 237-247
[6] Poplawski J V, Peters S, Zaretsky E V 2001 *Tribology Transactions* vol 1 (comparision of bearing life theories) pp 339-350
[7] Guo Z S, Zhang S H, and Zhang H 2014 *Advanced Materials Research* vols pp 1030-1032
[8] Wang Z W, Miao L J, Meng L Q 2014 *Coal Mine Machinery* vol 35 No.6 pp 85-89
[9] Wang M Y, Liu Q, Yang M Q, Gao W Z 2017 *Technology Innovation and Application* vol 3 pp 29-31
[10] Shu H Y, He C Z, Yuan H C, Jia H R 2016 *Coal Mine Machinery* vol 37 No.6 pp 68-71
[11] Hahn G T, Bhargava V, Rubin C A, Chen Q and Kim K 1987 *Journal of Tribology* vol 109 pp 618–626
[12] Liu D, M Yan, Jin H, Zou B 2015 *Journal of Mechanical Transmission* vol 39 No.9 pp 129-132